Noname manuscript No.
(will be inserted by the editor)

Intraoperative Optimization of Seed Implantation Plan in Breast Brachytherapy

Wanyu Liu[1,2] · **Jay Carriere**[1] · **Tyler Meyer**[3] · **Ron Sloboda**[4] · **Siraj Husain**[3] · **Nawaid Usmani**[4] · **Zhiyong Yang**[2] · **Mahdi Tavakoli**[1]

Abstract PURPOSE: Low-dose-rate permanent-seed (LDR-PS) brachytherapy has shown great potential for treating breast cancer. An implantation scheme indicating the template pose and needle trajectories is determined before the operation. However, when performing the pre-planned scheme intraoperatively, a change of the patient's posture will cause seed placements away from the desired locations. Hence, the implantation scheme should update based on the current patient's posture. METHOD: A numerical method of optimizing the implantation scheme for the LDR-PS breast brachytherapy is presented here. The proposed algorithm determines the fewest needle trajectories and template poses for delivering the seeds to the intraoperative desired locations. The clinical demand, such as the minimum distance between the chest wall and the needle, is considered in the optimization process. RESULTS: The method was simulated for a given LDR-PS brachytherapy procedure to evaluate the optimal scheme as the number of the template poses changing. The optimization parameters of the needles' number and the implantation errors are used to adjust the algorithm outcome. The results show, that the implantation schemes obtained by our method have a satisfactory accuracy in the cases of 2 or 3 template poses. The computation time is about 76s to 150s

Wanyu Liu · Jay Carriere · Mahdi Tavakoli (Corresponding Author)
[1] Department of Electrical and Computer Engineering, University of Alberta, 9211, 116 St NW, Edmonton, AB, T6G 1H9, Canada
E-mail: mahdi.tavakoli@ualberta.ca

Wanyu Liu · Zhiyong Yang
[2] School of Mechanical Engineering, Tianjin University, No. 135, Yaguan Road, Jinnan District, Tianjin, 300354, China

Tyler Meyer · Siraj Husain
[3] Division of Radiation Oncology, Tom Baker Cancer Centre, 331 29th St NW, Calgary, AB, T2N 4N2, Canada

Ron Sloboda · Nawaid Usmani
[4] Department of Oncology, Cross Cancer Institute, 11560 University Avenue, Edmonton, AB, T6G 1Z2, Canada

according to the number of the template poses from 1 to 3. CONCLUSIONS: The proposed method can find the optimal implantation scheme corresponding to the current desired seed locations immediately once there is a change of patient's posture. This work can be applied to the robot-assist LDR-PS breast brachytherapy for improving the operation accuracy and efficiency.

Keywords breast brachytherapy · low-dose-rate permanent-seed implantation · implantation scheme · insertion plan · template

1 Introduction

Breast cancer is the most commonly diagnosed type of cancer in women in Canada, where 1 in 8 women are expected to develop breast cancer during her lifetime[5]. Mastectomy and lumpectomy are two available breast cancer treatments. In mastectomy, the entire breast is removed. In lumpectomy, only the tumor and a portion of the adjacent breast tissue are surgically removed. A seroma (a pocket of bodily fluid that develops where the tumor was removed) and surrounding tissue, which is called the planning target volume (PTV), need to be irradiated to prevent a recurrence of cancer. Lumpectomy followed by external beam radiation therapy (XRT), therefore, is the more popular treatment [11].

XRT, the entire breast is treated using high-energy X-rays for 16-25 daily sessions lasting 3.5-7 weeks [3], thus the patient has to go round-trip between the home and the hospital for a long period. This treatment schedule can be a large burden for the patients bearing a long travel distance [2] and side-effects, such as acute skin reactions and painful skin breakdown, are frequent [17]. Low-dose-rate permanent-seed (LDR-PS) breast brachytherapy is an emerging follow-up radiation treatment to lumpectomy, providing an attractive option replacing XRT [20,16]. During this procedure, a needle containing radioactive seeds is supported by a guide template, which has a matrix of equidistant holes that the needle passes through, to implant the seeds at the pre-planned desired locations with ultrasound (US) guided; see Fig. 1. Compared with XRT, this treatment can reduce the overall treatment time, as it requires a maximum of one planning session and one implantation session, and can have better cosmetic outcome compared with skin lesions caused by XRT [12,21].

The procedure of LDR-PS breast brachytherapy is similar to prostate brachytherapy. The difference of this procedure over prostate brachytherapy is that the US probe can move freely on the surface of the breast. Additionally, in LDR-PS breast brachytherapy, the guide template grid is not rigidly attached to the US probe and can therefore be freely oriented, or reoriented, according to the operative demand.A general workflow for an LDR-PS breast brachytherapy operation is shown as Fig. 2. A CT-based planning session is done preoperatively with the patient supine with the arm lifted above the head. The seroma is segmented from the CT-images by a clinician and used to create the PTV for the dosimetry plan. The desired seed locations and the
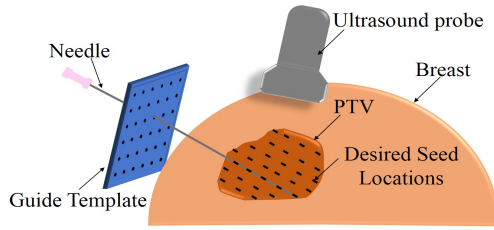
Fig. 1: LDR-PS breast brachytherapy setup with ultrasound probe and guide template.
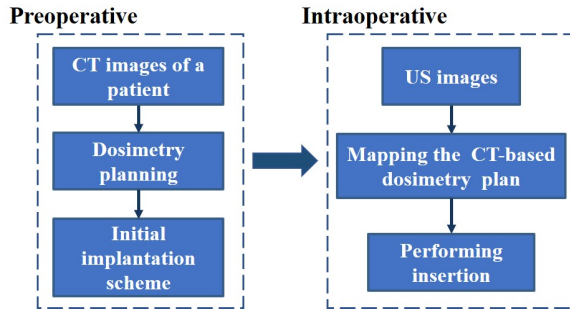

Fig. 2: General workflow of LDR-PS breast brachytherapy.

preoperative implantation scheme, which specifies the desired needle trajectories and the position and orientation ("pose") of the guide template, will be generated by the CT-based dosimetry plan.During implantation session, the patient keeps supine and the arm was abducted at $90°$. The CT-based dosimetry plan is registered to the current breast posture using US image, and the template is manually positioned to align the seed-implantation task indicating the desired seed locations and the implantation scheme in the intraoperative frame. Intraoperatively, a clinician performs seed implantation according to the implantation scheme with live US image feedback confirming that the needle is following the correct trajectory. At present workflow, the template only has one pose as the manually positioning process is very complex.

Optimally, the needle should not deflect during insertion, and it should be easily visible in the live US images. A review in [18] has shown that the problem with needle steering has been well addressed, with the help of robotics. The robot can perform the optimal needle rotation strategy to minimize the needle deflection. In our previous work, we developed US-guided needle steering methods and systems, which can be used in robot-assisted LDR-PS breast brachytherapy procedures, to make the needle insert along a desired straight trajectory inside the tissue [14, 10, 7, 8]. We also developed a system using autonomous US scanning for minimizing the tissue deformation [6] and tracking the needle accurately [1]. These developed robotic technologies can assist

LDR-PS breast brachytherapy. One more potential benefit of robotics for this procedure is that can replace the complex human operations for template positioning thus more than one poses of the template can be chosen to improve seed-implantation accuracy.

However, there is a complication in that there will be a change in pose of breast between the preoperative CT-scan and the intraoperative procedure as the patient's posture changes. This causes the desired seeds location changing thus difficulty in aligning the CT-based implantation scheme to the intraoperative seed-implantation task. Additionally, the pressure applied by the US probe on tissue affects needle tracking and tissue deformation. If the change of patient's posture is large or if there is tissue deformation, it becomes more challenging insert the needles to implant the seeds to match the preoperative plan. Because of this, the LDR-PS breast brachytherapy procedure is challenging even for experienced clinicians, which has hindered its adoption.

To address the challenges posed above, the preoperative implantation scheme should be updated, in a timely manner to match the current breast posture during or immediately before the intraoperative procedure. To this end, assuming the needle can go along a desired straight trajectory and be tracked accurately, we will propose a method to quickly optimize and update the implantation scheme for robot-assisted or manual LDR-PS breast brachytherapy in this work. The optimal implantation scheme can give the best template pose with the fewest required needle insertions while minimizing seed-implantation inaccurately. Our proposed method can be used and reused immediately when the patient's posture changes, or tissue is deformed, before or during the operation.

The paper is organized as follows. Section 2 introduces the method to plan and optimize the implantation scheme for the seed-implantation task. Section 3 provides a simulation-based example of a seed-implantation task using the proposed replanning method. The simulation results are displayed in Section 4. In Section 5 we discussed about the application of our method. Finally, concluding remarks and future work are provided in Section 6.

2 Method

The grid template used in LDR-PS breast brachytherapy has 13×13 guide holes with a $5\ mm \times 5\ mm$ grid resolution. Preoperatively, based on a chosen initial template pose in CT images, the clinician makes the needle insertion plan specifying the seeds carried by a needle and desired needle trajectory for the seed-implantation task. The seed-implantation task is to deliver the seeds into the PTV at locations indicated within the CT volume. The PTV is cropped to not include the skin and chest wall. A seed-implantation task generally is based on several planning images that have desired seed locations, as Fig. 3 shows.

These planning images are generated from the preoperative CT volume, which are perpendicular to the given template plane. Each planning image
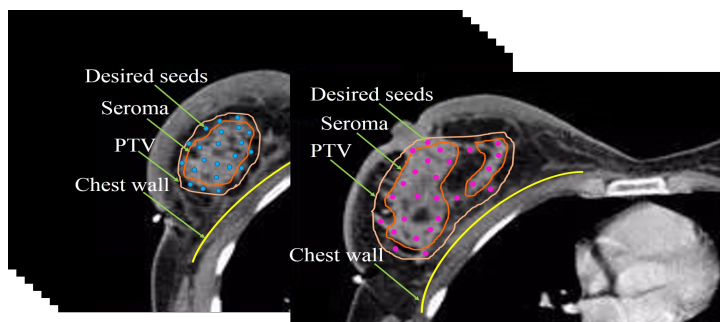
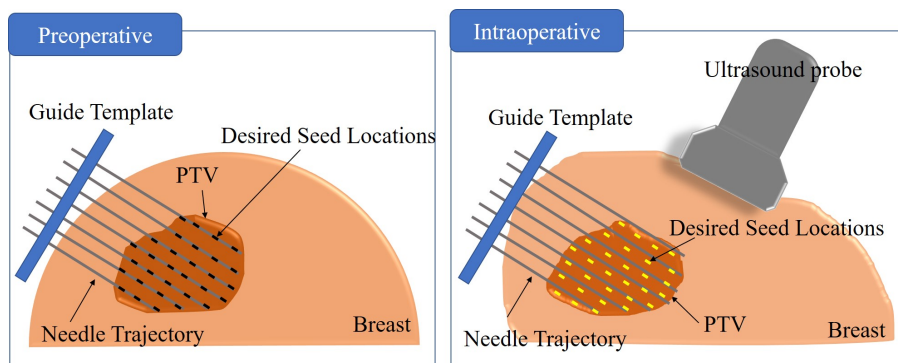Fig. 3: Seed-implantation task in the CT volume.

Fig. 4: Tissue deformation and change of breast posture affect seed desired locations.

will now have a row of guide holes corresponding to it. Needles will be inserted through the paths guided by some of these holes to deliver the seeds to the desired locations intraoperatively. Hereby, the initial implantation scheme, which contains all preoperative planning needle insertion plans and the given template pose, is determined.

However, during the operation, the breast posture will be changed due to gravity once the patient posture changed, and the breast tissue will be deformed by the US probe. Thus, the desired seed locations will only be aligned for the preoperative CT breast posture. The pre-planned needle trajectories may not be possible to follow intraoperatively, see Fig. 4. Our method is to replan the optimal implantation scheme for delivering the seeds to the intraoperative desired locations, where they were obtained by registering the pre-planned locations to the current patient's posture by US-image. The optimal implantation scheme will specify the best template poses and needle insertion plans, which indicate all desired needle trajectories.

There will be many possible implantation schemes that can achieve the seed-implantation task when choosing different guide holes in the template or
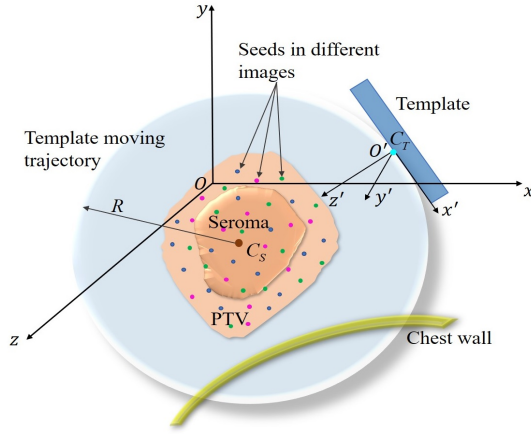
Fig. 5: Template positioning in the 3D space.

moving the template around the PTV. Next, we will introduce our proposed method of planning an optimal implantation scheme.

2.1 Implantation Scheme Planning

A base frame $\{O\}$, with axes x, y, and z, is built on the patient's body and indicates the relative pose of other elements in the operation system. The $x-y$ plane is parallel to the planning plane. Another coordinate system $\{O'\}$, with axes x', y', and z', is built on the center of the template to indicate the template pose, as Fig. 5 shows.

The orientation of the frame $\{O'\}$ is determined by $\{O\}$ rotating α degrees around its z-axis and then rotating $90°$ around the x-axis of the rotated frame, following the right-hand rule. When the value of α is given, the template pose will be determined. The rotation matrix from the template frame $\{O'\}$ to the base frame $\{O\}$ is defined as follow:

$$_{O'}^{O}R = R(z, \alpha) \cdot R(x, 90°) = \begin{bmatrix} \cos\alpha & 0 & 1 \\ \sin\alpha & 0 & -\cos\alpha \\ 0 & 1 & 0 \end{bmatrix} \tag{1}$$

Because the template plane is always perpendicular to the planning image, the template can be thought of as a line segment by projecting it onto the $x-y$ plane. The midpoint of the line segment moves along a circular trajectory with radius R surrounding the PTV to ensure all seeds are contained in areas that the needle can reach. The line segment is tangent to the circular trajectory at its midpoint, which is marked as C_T in Fig. 5. Knowing the location of $\{O'\}$ in $\{O\}$, we are able to calculate the positions of all grid holes in frame $\{O\}$.

For one or more given values of α, there are many possible needle paths determined by guide holes that can be chosen for delivering the seeds to the
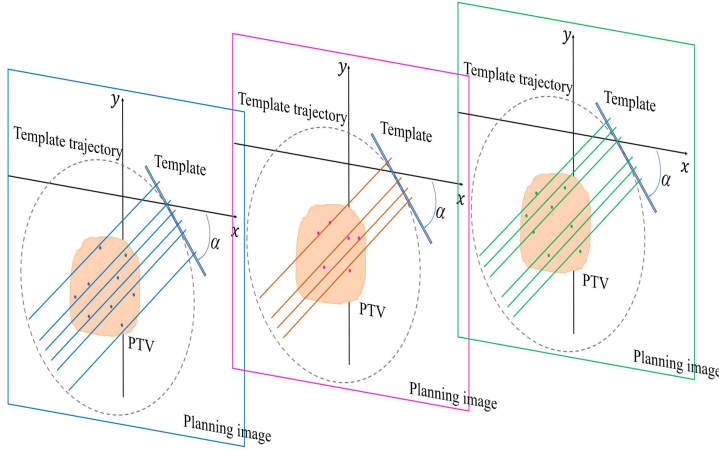
Fig. 6: Implantation scheme for a seed-implantation task

desired locations in a planning plane. To minimize implantation errors, each seed will be assigned to the most closest needle path to its desired location. The chosen needle paths based on the template pose(s) determined by the given angle(s) α, therefore, constitute an insertion plan for the corresponding image. Designing an implantation scheme is that searching needle path lines determined by the guide holes given by the value of α for the template poses in each planning image. A complete needle implantation scheme likes shown in Fig. 6, where different colors denote the various planning images and needle path lines.

The diameter and the center point of the template circular trajectory are denoted as L and $C_S(X_s, Y_s)$, respectively. L is determined by effective length of a needle and $L = 2R$. (X_s, Y_s) is the coordinate of C_S which is given by $C_S = (P_I + P_{II})/2$. P_I is the location of seed I, which is the farthest one from the origin O, and P_{II} is the location of the farthest seed from the seed I. For a given α, the location (X_t, Y_t) of C_T can be calculated as:

$$\left.\begin{array}{l} X_t = \frac{L}{2}\cos(\alpha + \frac{\pi}{2}) + X_s \\ Y_t = \frac{L}{2}\sin(\alpha + \frac{\pi}{2}) + Y_s \end{array}\right\} \tag{2}$$

While, the locations of guide holes $C_h(X_h, Y_h)$, $h = 1, \ldots, 13$, are

$$\left.\begin{array}{l} X_h = X_t - 5(7 - h)\cos\alpha \\ Y_h = Y_t - 5(7 - h)\sin\alpha \end{array}\right\} \tag{3}$$

Then, the equation of needle path line determined by the guide hole h can be expressed as:

$$l_h = (x - X_h)\tan(\alpha + \frac{\pi}{2}) + Y_h, \ \ h = 1, \ldots, 13 \tag{4}$$

For a seed-implantation task, the total number of planning images is denoted as N, and each planning image n, $1 \leq n \leq N$, contains S_n seeds. The

location of the j seed in the planning image n is marked as $P_{j^{(n)}}(x_{j^{(n)}}, y_{j^{(n)}})$, where $j = 1, \ldots, S_n$. The total seeds number of a seed-implantation task are denoted by $\mathbf{S_N} = [S_1, S_2, \ldots, S_n, \ldots, S_N]$. The squared distance between the seed j in image n and each line l_h is calculated as follows:

$$d_{j^{(n)}, h_\alpha}^2 = \frac{[x_{j^{(n)}} \tan(\alpha + \frac{\pi}{2}) - y_{j^{(n)}} - X_{h_\alpha} \tan(\alpha + \frac{\pi}{2}) + Y_{h_\alpha}]^2}{\tan(\alpha + \frac{\pi}{2})^2 + 1} \tag{5}$$

The minimum of $d_{j^{(n)}}^2$ is the implantation squared error of the seed $P_{j^{(n)}}$, which is denoted as $e_{j^{(n)}}^2$. The corresponding hole is denoted as $h_{\alpha, j^{(n)}}$, which is selected for implanting the seed $P_{j^{(n)}}$. With recording the template pose, the selected hole, and the implantation squared error, the insertion plan for seed j in planning image n is

$$M_{j^{(n)}} = \left[\alpha \ h_{\alpha, j^{(n)}} \ e_{j^{(n)}}^2 \right] \tag{6}$$

The insertion plan of all seeds in planning image n is given by

$$\mathbf{M_n} = \left[M_{1^{(n)}} \ldots M_{j^{(n)}} \ldots M_{S_n^{(n)}} \right]^T \tag{7}$$

Finally, the implantation scheme for implanting all seeds are recording by a block matrix:

$$\mathbf{M} = \left[\mathbf{M_1} \ldots \mathbf{M_n} \ldots \mathbf{M_N} \right]^T \tag{8}$$

For one or more given $\alpha(s)$ of an implantation scheme, the matrix $\mathbf{M}$ will always reserve the needle paths with the minimum implantation error for each seed. A method for optimizing the implantation scheme specifying the best template poses and the desired needle trajectories is developed in the next section.

2.2 Implantation Scheme Optimizing

There are two main factors that we will consider for optimization, which as they add operating time and complexity to a brachytherapy procedure. The first is trying to minimize movement or relocation of the template and the second is to try to minimize the number of inserted needles. The purpose of our optimization method is to find a satisfactory implantation scheme that involves the fewest number of needles for a number of template poses and can accurately implant seeds.

An additional condition that needs to be considered when selecting an implantation scheme is that the needle trajectories should not pass too close to the chest wall. There are two possible situations will cause a risk of the needle passing too close to the chest wall (possibly puncturing it): The first one is that the template pose is outside of a reasonable range so that the lowest needle path is too close to the chest wall, as shown in Fig. 7a; the second one is when the template is placed inside the reasonable range the distance between
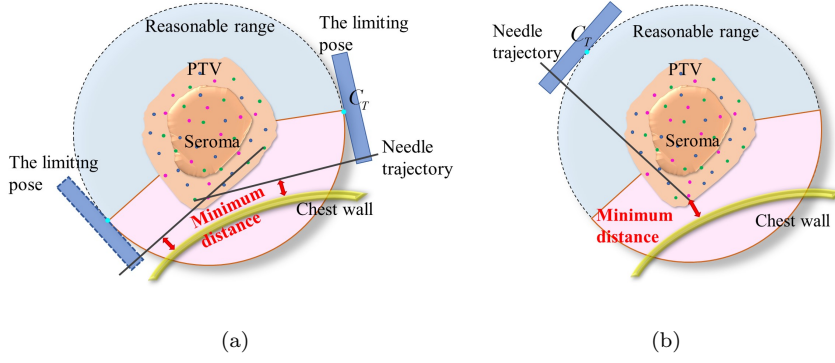
Fig. 7: Two situations of causing the risk of needle puncturing the chest wall. (a) The template moving outside of the reasonable range; (b) The minimum distance between the needle tip and chest wall is less than the desired safe value

the needle tip (delivering the lowest seeds) and the chest wall is too small, see Fig. 7b. Hence, the template pose should be both in a reasonable range and ensure that the minimum distance between the needle trajectories and the chest wall is greater than a safe value.

To optimize a implantation scheme $\mathbf{M}$, the cost function is designed as follow:

$$\mathcal{F}_{(N,\mathbf{s_N})} = w_1 \sum_{n=1}^{N} \sum_{j=1}^{S_n} \frac{e_{j^{(n)}}^2}{\sum_{n=1}^{N} S_n} + w_2 A + w_3 \frac{B}{\sum_{n=1}^{N} S_n} \qquad (9)$$

where A and B are the total numbers of template poses and needles of a implantation scheme, respectively. Changing the weight parameters w_1, w_2, and w_3, allows for emphasizing the importance of the implantation error, the total number of times the template is re-positioned, and the total number of needle insertions, respectively.

Based on clinics-operational requirements, we can limit A to be between a maximum number A_{max} and a minimum number A_{min}. A value range $\Lambda = [\alpha_0, \alpha_1]$, is given to α to make sure the template will only be placed in the feasible circular trajectory. The minimum distance from a needle trajectory to the chest wall is denoted as d_{min}, and it should be greater than the safe value d_{safe}. The optimization problem for a complete implantation scheme is

$$\text{minimize } \mathcal{F}_{(N,\mathbf{s_N})} = w_1 \sum_{n=1}^{N} \sum_{j=1}^{S_n} \frac{e_{j^{(n)}}^2}{\sum_{n=1}^{N} S_n} + w_2 A + w_3 \frac{B}{\sum_{n=1}^{N} S_n}$$

$$\text{subject to } A_{min} \leq A \leq A_{max}, \ \alpha \in \Lambda, \text{ and } d_{min} \geq d_{safe}$$

As the template has 13×13 holes, there will be 169 possible needle paths for implanting a seed every time changing the template pose. Simulated Annealing (SA) algorithm is a probabilistic technique for approximating the global minimum in a large search space of a given function in a reasonable amount of time [9,13].
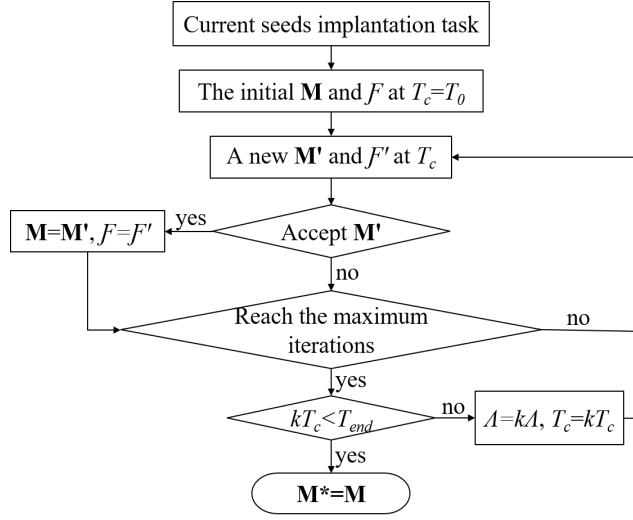
Fig. 8: The simulated annealing algorithm flowchart for optimizing the needle implantation scheme.

SA algorithm works as the temperature progressively decreases with rate k from a initial temperature T_0 to a final temperature T_{end}. Here we use the SA method for searching the optimal implantation scheme $\mathbf{M}^*$. As Fig. 8 shows, the algorithm is as follow:

(1) At the beginning, T_0 is assigned to the algorithm. The algorithm generates a random value of α to plan an initial implantation scheme $\mathbf{M}$, and the cost value $\mathcal{F}$ of $\mathbf{M}$ is calculated.

(2) The algorithm is then passed through a cooling process in a step manner. At each temperature, algorithm will generate new solutions $\mathbf{M}'$ and calculate the corresponding costs $\mathcal{F}'$ repeatedly. The algorithm will accept the new scheme of each temperature with the probability p instead of the old one, where

$$p = \begin{cases} 1 & \text{if } \mathcal{F} > \mathcal{F}' \\ exp(-\frac{\Delta}{T_c}) & \text{if } \mathcal{F} \leq \mathcal{F}' \end{cases}$$

where Δ is the difference between the cost of the new and the old schemes at the current temperature T_c.

(3) The algorithm lowers the temperature using $T_c = kT_c$ for next computing step. At each step, the best implantation scheme found so far is stored while the rang of α is reduced with the rate k using $\Lambda = k\Lambda$ for the next step, therefore Λ will gradually approaching to the optimal solution.

(4) The algorithm stops if the temperature of the next step will lower than T_{end}.

3 Simulation

The optimization algorithm needs to balance the implantation error and operational complexity by adjusting the cost function's weight parameters. To find reasonable weights, a virtual example consisting of 100 desired seed locations, which are randomly distributed with a space greater than 1 cm in 5 planning images, is used in the simulation. These locations shown in the images are considered as the intraoperative desired which have been registered by US image for matching the current patient's posture. The implantation task for this simulation is to deliver the seeds to the locations indicated in the 5 planning images.
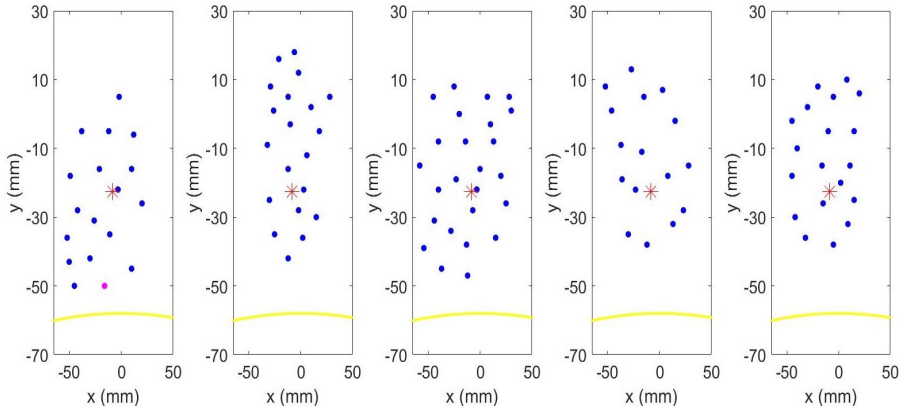

Fig. 9: A virtual implantation task with 100 seeds across in 5 images.

For this simulation, we set $L = 120$, because 120mm is the average needle insertion depth observed in clinical breast brachytherapy operations. The available range of α is $\Lambda = [-60°, 60°]$, to ensure the template is always positioned above the patient. Meanwhile, the safe value d_{safe} is set as 5mm to avoid the needle going too close to the chest wall. The seed-implantation task is shown in Fig. 9, where the red star is the center point of the circular template trajectory, the yellow curve represents the chest wall, and the pink point is the seed closest to the chest wall.

This simulation has three scenarios which are respectively set the template pose number A equals to 1, 2, and 3, therefore, we can make $w_2 = 0$ and then only focus on the effect of changing w_1 and w_3 has on the optimized implantation scheme. We will evaluate the needles' number and the implanting Root Mean Square Errors (RMSEs) of the optimal implantation schemes concerning the varying w_1 and w_3. The simulation process is programmed and implemented in Matlab 2019a (The Mathworks Inc, Natwick, MA, USA).

4 Results

The simulation results of each scenario, including the needles' number and the implanting RMSE of the optimal implantation scheme adjusted by setting different optimizing parameters w_1 and w_3, are evaluated in this section.

Fig. 10a shows the needles' number and the RMSE of the optimal implantation scheme varying with w_1 and w_3 when there is only one template pose. The optimal implantation scheme is sensitive to the varying values of w_1 and w_3 when $4 \geq w_1 \geq 1$ and $200 \geq w_3 \geq 60$. When $10 \geq w_1 \geq 5$, the implantation RMSEs and the number of needles of an optimal implantation scheme are tend to be stabilized.

As Fig. 10b shows, in the case of that there are two template poses in an implantation scheme, the results are sensitive to the varying values of w_1 and w_3 when $20 \geq w_1$ and $w_3 \geq 20$. Adjusting w_3 will only affect the needles' number without significant decrease the implantation RMSEs as $w_1 \geq 20$.

The optimal implantation scheme, which has three template poses, always can provide good needle trajectories for all seeds, see Fig. 10c. Adjusting w_1 and w_3 have significant effect on needles' number but not on RMSEs. When $w_1 \geq 20$, the optimal implantation schemes all can have a very small implantation error, while the needles' number still has a big flexible range to be adjusted.

5 Discussion

From the results shows above, the proposed method can optimize the implantation scheme by adjusting the weight parameters. The computation outcomes of the optimal insertion schemes with three cases are compared in Table 1. According to the survey, the mean implantation error performed by experienced clinicians manually is about 6.3mm[19]. Even for the prostate biopsies, the average errors are about 5.5 to 6 mm by using a rigid needle [4,22]. However, the smallest seroma visible in US images is about 2mm [15]. In the clinical, the implantation error is expected to lower than 3mm. As shown in Table 1, the optimal implantation schemes with two or three template-poses conform to the clinical requirements. In contrast, the case with only one pose makes no satisfactory performance enough.

In each calculating loop, the algorithm searches the best needle trajectory from all paths provided by the given template poses for every seed. Hence, setting more template poses will cost more computation time, while fewer seed locations in a task make less computation time. We performed the simulation only with the maximum number of template poses was 3, as the accuracy of the optimal implantation scheme had been good enough in that case. Additional template poses will increase computation time significantly but not improve the accuracy of scheme. The computation time of optimizing the implantation scheme for our example is about 76s to 150s respecting 1 to 3 template poses.
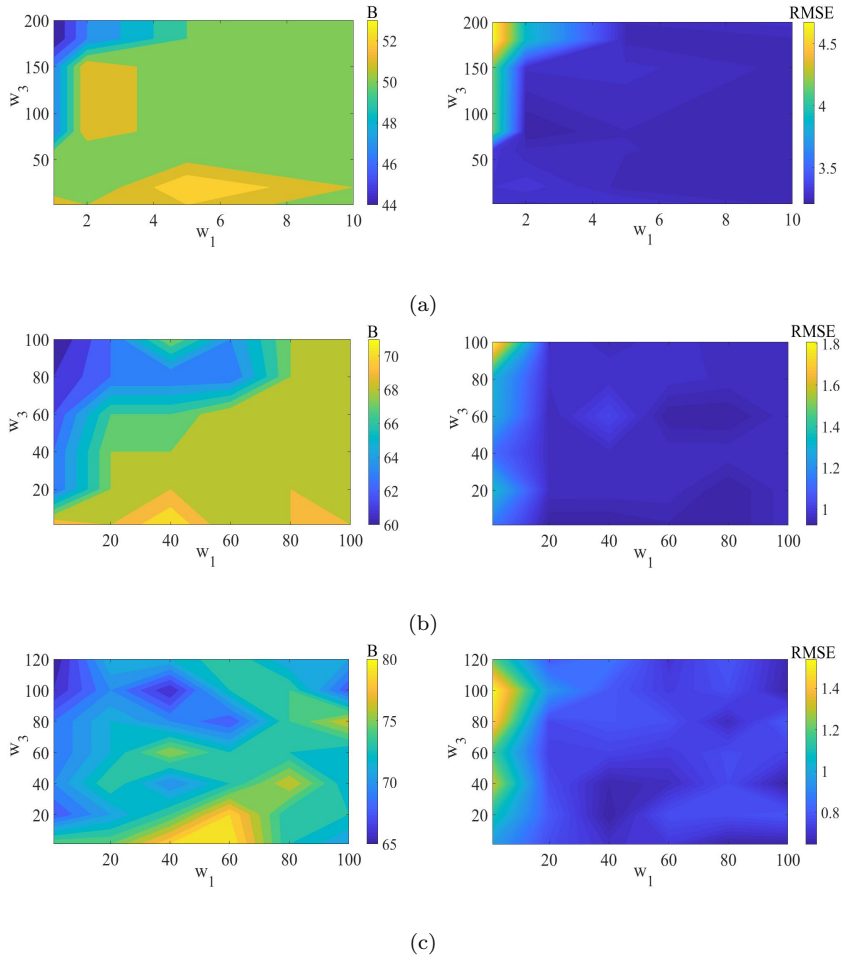
(a)

(b)

(c)

Fig. 10: The Needle number and RMSEs of optimal implantation schemes adjusting by the weight parameters.(a) The case of one template pose; (b) The case of two template pose; (c) The case of three template pose

Considering the result for this huge implantation task, which contains 100 seed locations, the efficiency of the algorithm is satisfactory.

The method can quickly find a good enough implantation scheme for a seed-implantation task, which makes it possible to immediately update the optimal implantation scheme according to the current patient's posture during the operation. The scheme indicated the explicit pose of the template in the patient's frame. After registering the robot, the template can be positioned automatically and accurately during the operation process, thus improve surgical efficiency. In our method, the value of w_2 is related to the template-positioning time by a robot, which can be used to adjust the optimization outcome con-

Table 1: Computation outcomes of the optimal insertion schemes.

Number of template poses	The optimal implantation scheme		
	Needle number	RMSEs (mm)	Computation time (s)
1	44~52	3.18~4.67	76
2	62~71	0.92~1.33	107
3	65~80	0.65~1.30	150

sidering the robot performance. The scheme recorded the seed-implantation method (about the seeds carried by each needle, the needle trajectories, and insertion depths) mathematically, thus can easily be shown to clinicians by Augmented Reality (AR) technology for guiding needle insertion during the operation.

6 Conclusion

This work presented a method of planning and optimizing the implantation scheme for breast brachytherapy. The optimal implantation scheme can determine the best template poses and the fewest desired needle trajectories to accurately implant the seeds at their desired locations. A simulation was performed on a given seed-implantation task, which contains 100 seeds in 5 planning images, to evaluate the effect of the weight parameters of the needles' number and RMSEs on the optimal implantation schemes with the number of template poses from 1 to 3 respectively. The results show the relationship and the effective value range of these weight parameters when balancing the implantation error and the operative complexity. The parameters can be set according to the clinical requirement. Our proposed method is only processed based on the desired seed locations and operating conditions and it can be immediately used to find the optimal implantation scheme with respect to the patient's intraoperative posture.

The future work involves combining this work with robot-assisted breast brachytherapy and AR technology. Taking the advantages of rapid, accurate and repeatable actions of a robot, it will achieve automatic template positioning, which can significantly reduce the operating burden of clinicians. The optimal implantation scheme can also be displayed by using AR technology to provide a visual reference for clinicians when doing an insertion training or a clinical operation. That can enhance situational awareness for clinicians and allow them to quickly evaluate seed placement accuracy during needle insertion. The seed-implantation experimental study will also be performed on a real tissue sample by integrating the proposed method with robot and AR setup to verify the assist effect of the system for LDR-PS breast brachytherapy.

Disclosure of potential conflicts of Interest

Conflict of Interest: The authors have no conflicts of interest to declare that are relevant to the content of this article.

Human and animal rights

This article does not contain any studies with human participants or animals performed by any of the authors.

Informed consent

This articles does not contain patient data.

References

1. Afshar, M., Carriere, J., Meyer, T., Sloboda, R., Siraj, H., Usmani, N., Liu, W., Tavakoli, M.: Autonomous ultrasound scanning to localize needle tip in breast brachytherapy. International Symposium on Medical Robotics (2020). Accepted
2. Athas, W.F., Adams-Cameron, M., Hunt, W.C., Amir-Fazli, A., Key, C.R.: Travel Distance to Radiation Therapy and Receipt of Radiotherapy Following Breast-Conserving Surgery. JNCI: Journal of the National Cancer Institute **92**(3), 269–271 (2000)
3. Bartelink, H., Horiot, J.C., Poortmans, P., Struikmans, H., Van den Bogaert, W., Barillot, I., Fourquet, A., Borger, J., Jager, J., Hoogenraad, W., Collette, L., Pierart, M.: Recurrence rates after treatment of breast cancer with standard radiotherapy with or without additional radiation. New England Journal of Medicine **345**(19), 1378–1387 (2001)
4. Blumenfeld, P., Hata, N., DiMaio, S., Zou, K., Haker, S., Fichtinger, G., Tempany, C.: Transperineal prostate biopsy under magnetic resonance image guidance: A needle placement accuracy study. Journal of magnetic resonance imaging : JMRI **26**, 688–94 (2007)
5. Canadian Cancer Society's Steering Committee: Canadian cancer statistics. http://www.cancer.ca/statistics (2019)
6. Carriere, J., Fong, J., Meyer, T., Sloboda, R., Husain, S., Usmani, N., Tavakoli, M.: An admittance-controlled robotic assistant for semi-autonomous breast ultrasound scanning. In: 2019 International Symposium on Medical Robotics (ISMR), pp. 1–7 (2019)
7. Carriere, J., Khadem, M., Rossa, C., Usmani, N., Sloboda, R., Tavakoli, M.: Event-triggered 3d needle control using a reduced-order computationally efficient bicycle model in a constrained optimization framework. Journal of Medical Robotics Research (2018)
8. Carriere, J., Khadem, M., Rossa, C., Usmani, N., Sloboda, R., Tavakoli, M.: Surgeon-in-the-loop 3-d needle steering through ultrasound-guided feedback control. IEEE Robotics and Automation Letters **3**(1), 469–476 (2018)
9. Carriker, W.F., Khosla, P.K., Krogh, B.H.: Path planning for mobile manipulators for multiple task execution. IEEE Transactions on Robotics and Automation **7**(3), 403–408 (1991)

10. Fallahi, B., Rossa, C., Sloboda, R.S., Usmani, N., Tavakoli, M.: Sliding-based image-guided 3d needle steering in soft tissue. Control Engineering Practice **63**, 34 – 43 (2017)
11. Fisher, B., Anderson, S., Bryant, J., Margolese, R.G., Deutsch, M., Fisher, E.R., Jeong, J.H., Wolmark, N.: Twenty-year follow-up of a randomized trial comparing total mastectomy, lumpectomy, and lumpectomy plus irradiation for the treatment of invasive breast cancer. New England Journal of Medicine **347**(16), 1233–1241 (2002)
12. Hepel, J.T., Arthur, D., Shaitelman, S., Polgár, C., Todor, D., Zoberi, I., Kamrava, M., Major, T., Yashar, C., Wazer, D.E.: American brachytherapy society consensus report for accelerated partial breast irradiation using interstitial multicatheter brachytherapy. Brachytherapy **16**(5), 919 – 928 (2017)
13. Khadem, M., Rossa, C., Sloboda, R., Usmani, N., Tavakoli, M.: Ultrasound-guided model predictive control of needle steering in biological tissue. Journal of Medical Robotics Research **01**, 1640007 (2016)
14. Khadem, M., Rossa, C., Usmani, N., Sloboda, R., Tavakoli, M.: Semi-automated needle steering in biological tissue using an ultrasound-based deflection predictor. Annals of Biomedical Engineering **45** (2016)
15. Moreira, P., Misra, S.: Biomechanics-based curvature estimation for ultrasound-guided flexible needle steering in biological tissues. Annals of biomedical engineering **43**(8), 1716—1726 (2015)
16. Pignol, J.P., Keller, B., Rakovitch, E., Sankreacha, R., Easton, H., Que, W.: First report of a permanent breast 103pd seed implant as adjuvant radiation treatment for early-stage breast cancer. International Journal of Radiation Oncology*Biology*Physics **64**(1), 176 – 181 (2006)
17. Rebecca Thorpe, H.D.S.: A literature review of the role of brachytherapy in the management of early-stage breast cancer. Journal of Radiotherapy in Practice pp. 1–10 (2019)
18. Rossa, C., Tavakoli, M.: Issues in closed-loop needle steering. Control Engineering Practice **62**, 55 – 69 (2017)
19. Taschereau, R., Pouliot, J., Roy, J., Tremblay, D.: Seed misplacement and stabilizing needles in transperineal permanent prostate implants. Radiotherapy and oncology : journal of the European Society for Therapeutic Radiology and Oncology **55**, 59–63 (2000)
20. Thorpe, R., Drury-Smith, H.: A literature review of the role of brachytherapy in the management of early-stage breast cancer. Journal of Radiotherapy in Practice pp. 1–10 (2019)
21. Vicini, F.A., Kestin, L., Chen, P., Benitez, P., Goldstein, N.S., Martinez, A.: Limited-Field Radiation Therapy in the Management of Early-Stage Breast Cancer. JNCI: Journal of the National Cancer Institute **95**(16), 1205–1210 (2003)
22. Vrooijink, G., Abayazid, M., Patil, S., Alterovitz, R., Misra, S.: Needle path planning and steering in a three-dimensional non-static environment using two-dimensional ultrasound images. The International Journal of Robotics Research **33**, 1361–1374 (2014)